

## Inter-annual variability of sea surface temperature, wind speed and sea surface height anomaly over the tropical Indian Ocean

P.M. Muraleedharan, T. Pankajakshan and P.V. Sathe  
National Institute of Oceanography, Dona Paula, Goa 403 004, India  
E-mail : murali@csnio.ren.nic.in

### Abstract

Being land-locked at the north, the Indian Ocean and its surrounding atmosphere behave in such a way that the ocean-atmosphere interaction over this domain is different from that over the other oceans, exhibiting a peculiar dynamics. The sparse data coverage over the Indian Ocean was one of the several reasons for the incomplete information accumulated to date. With the advent of satellite technology and advanced modeling techniques the availability of data with space and time became easier. Here we have made an attempt to study the annual and inter-annual variability of certain prominent processes occurring over the tropical Indian Ocean. The monthly mean values of Wind Speed (FSU), Sea Surface Temperature (REYNOLDS) and Sea Surface Height Anomaly (TOPEX/POSEIDON) over a period of 5 years from 1993 are used for this investigation. The first EOF mode of seasonal and non-seasonal data set gives annual and inter-annual variability over the tropics. A strong signal of dipole is observed in all the fields during 1994 and 1997 coinciding with the El Nino events. The reversal of westerlies at the equator appeared to be responsible for the formation of anomalous cooling and warming near Sumatra and Somali, respectively. The oscillation of westerlies from south to the equator and back and its association with the pre- and post-monsoon Equatorial Jet is evident over 62°E and 90°E. The amplitude of this oscillation is more at the eastern section. A propagation of high sea surface is noticed at both 62°E and 90°E from the equator to 25°S, which seems to be associated with the above meridional oscillation of the westerly wind. The time-longitude section at the north (10°-15°N) and south (10°-15°S) exhibits the propagation of Rossby waves.

### 1. Introduction

The Indian Ocean is land-locked at its north, a unique feature in comparison to the Pacific and the Atlantic, by virtue of which it experiences differential heating resulting in enhanced atmospheric dynamics, which ultimately affects the underlying ocean. The frequent reversal of wind (monsoon) is one such phenomenon paving way for the formation of monsoon drift current during the monsoon season and the inter-monsoon Equatorial Jet (Muraleedharan, 1995), a unique feature discovered by Wyrtki (1973) more than two decades ago. The dynamics of this domain is further complicated by the proximity of the abnormally high saline Persian Gulf and Red Sea waters in the north-west (Arabian Sea) and the desalination process occurring by the enhanced river runoff at the northeast (Bay of Bengal). The different climatic condition of these two regions makes one (Arabian Sea) more susceptible to evaporation, a process that serves to augment the already high surface salinity, while the other (Bay of Bengal) receives excessive precipitation which leads to further freshening of the surface water. These features demarcate two independent domains, each supporting a dynamics of its own.

The remarkable meridional shift in the thermal equator (ITCZ) further complicates the dynamics of this

part of the world ocean. The equatorial warm pool and its association with the ITCZ is also well known (Rao et al., 1989; Shenoi et al., 1999). The disappearance of the warm pool near Sumatra and the formation of abnormally low sea surface temperatures are found to be associated with the remarkable warming near the Somali region and the process is often referred to as Indian Ocean dipole (Shaji et al., 1999). Although there are indications of its association with the El Nino-La Nina event (Chambers et al., 1999), Shaji et al. (1999) and Webster et al. (1999) believe that it is an expression of internal dynamics rather than a direct response to external influence.

The oceanic response to changes in atmospheric forcing leads to the formation of planetary waves such as the Kelvin and Rossby waves. The equatorial Kelvin waves, upon impinging on the west coast, have been shown to be able to generate poleward propagating coastal Kelvin waves (Moore, 1968; Anderson and Rowlands, 1976; Clarke, 1983). Poleward propagating Kelvin waves along the coast of North America have been shown to excite Rossby waves (Johnson and O'Brien, 1990). The consistent suppressing of upwelling at the east coast of India is often attributed to the westward propagating Rossby waves generated from the northward propagating coastally trapped Kelvin wave (Sengupta, personal communication).

The present paper is an attempt to unveil the inter-annual variability of some of these dominant processes over a period of 5 years (1993 – 1997) by analyzing parameters primarily associated with any oceanic processes *viz*; wind speed, sea surface temperature and sea surface height anomaly. The following section deals with the details of the data used and the method of analysis adopted to achieve the objectives. The results derived are discussed in the last section.

## 2. Materials and Methods

The parameters closely associated with the ocean dynamics are Wind Speed (WS), Sea Surface Temperature (SST) and Sea Surface Height (SSH). The satellite mounted sensors are now capable of measuring these parameters with sufficient accuracy. The added advantage of satellite derived products is the synoptic coverage with space and time. The sea surface temperature data products used here were generated by combining satellite and *in situ* measurements optimally interpolated to a 1° grid (Reynolds and Smith, 1994). The Florida State University (FSU) winds were produced by combining all available wind measurements from ships, buoys and other oceanic sites and are averaged into monthly 1° grids for the Indian Ocean (Goldenberg and O'Brien, 1981). The wind stresses are converted into wind speed and direction and then further converted to zonal and meridional components. The sea surface height anomaly data from the TOPEX/POSEIDON altimeter (Jan. 1993 – Dec. 1997) were used to investigate the oceanic response to the atmospheric forcing. The rms accuracy of SSH retrieval is about 2-3 cm based on comparison with tide gauges (Chambers et al., 1998; Cheney et al., 1994).

The size of the data matrix is from 40°E to 120°E and 25°N to 25°S. The SST and FSU winds are available at 1°x 1° latitude-longitude bin while the SSH is 1°x4° latitude-longitude bin. As a first stage the data were subjected to the Empirical Orthogonal Function (EOF) analysis to understand the significant modes. In order to analyze the annual and inter-annual modes separately, the data sets are divided into seasonal (annual

features) and non-seasonal (inter-annual features) deviation data sets. Seasonal deviations have been obtained by subtracting long term mean of 5 years from each individual monthly mean and for non-seasonal deviations the long-term monthly mean have been subtracted from each individual month.

The spatial demeaning is performed along the equator, after calculating the longitudinal mean (between 2.5°N & S for all the parameters) for preparing time-longitude plots to understand the propagating forces along the equator. Similar procedures were followed to prepare the time-longitude plots at 15°N (10°–15°N) and 15°S (10°–15°S). Time-latitude sections were also taken along 62°E and 90°E to understand the processes occurring across the equator in the Arabian Sea and Bay of Bengal domains.

## 3. Results and Discussion

### 3.1 Annual and inter-annual variability

The data matrix of each parameter (WS, SST and Sea Surface Height Anomaly (SSHA)) is separated into seasonal deviation data set and non-seasonal deviation data set by removing inter-annual and annual signals, respectively. These data sets are then separately subjected to EOF analysis. Table 1 shows the closeness ratio of first five modes. The first mode of seasonal and non-seasonal data set, as seen from the closeness ratio, is significant compared to the subsequent modes and hence the study is based on the first mode to address the seasonal and non-seasonal signatures of the data.

### 3.2 Annual signature

The spatial and temporal variability of the annual signal as represented by the 1<sup>st</sup> EOF mode of the seasonal deviation data set is given in Fig. 1. The variation of the zonal wind component (upper panel in Fig. 1) indicates a belt of westerlies and easterlies centered around 8°N & 8°S, respectively, right across the Indian Ocean during the northern hemisphere summer (June-Aug), (henceforth the term summer/winter refers

**Table 1.** Closeness ratio (in %) of different modes obtained from single value decomposition of Sea Surface Temperature (SST), Wind Speed (FSU) and Sea Surface Height Anomaly (SSH)

Modes	SST		FSU (Ucomp)		SSH	
	Seasonal	Non-Seasonal	Seasonal	Non-Seasonal	Seasonal	Non-Seasonal
1	67.5	26.4	69.3	28.7	16.2	21.6
2	20.2	13.5	7.3	8.9	15.7	9.6
3	3.3	12.0	6.1	7.6	13.5	7.1
4	2.2	6.3	2.4	6.0	5.7	4.6
5	1.1	4.8	1.6	4.1	4.7	3.9

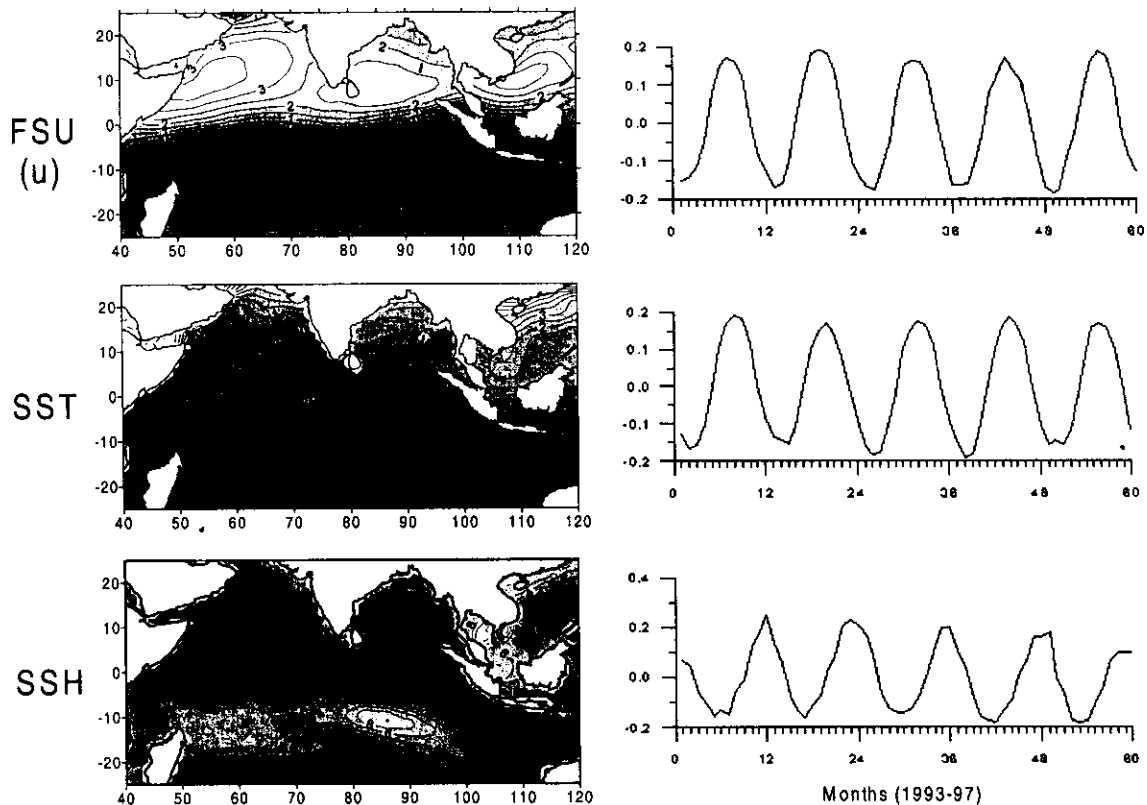


Fig 1. First spatial (left panel) and temporal (right panel) EOF mode of seasonal Deviation data. U-component of the wind speed (upper panel), Sea Surface Temperature (middle panel) and Sea Surface Height Anomaly (bottom panel).

to northern hemisphere summer/winter). The winds are reversed during the winter season (Dec- Feb). The SST variability map also exhibits warming and cooling of the northern Indian Ocean during the summer and winter seasons, respectively. The southern Indian Ocean behaves just opposite to its northern counterpart, as indicated by the temporal oscillation of the amplitude (middle panel in Fig. 1). It is interesting to note that the western equatorial Indian Ocean is warmer than the eastern half during the summer months and cooler in the winter months. On the contrary the SST distribution shows cooling along the coast of Somali and the southwest coast of India during summer and warming in winter. The spatial and temporal modes of the SSHA indicate higher sea surface at the north during May-Aug and lower sea level south of the equator, which reverse during Nov-Feb (lower panel in Fig. 1). There is a patch of low sea level along the southwest coast of India during the summer season. The east coast sea level is abnormally low during the winter season. There is a long patch of high sea level along the equator from 70°-90°E during the pre-monsoon months and it seems to be associated with the tongue protruding from the south of Indonesia.

The zonal wind pattern during the June-Aug. period represents the monsoon wind which has a strong east-west component in the southern hemisphere and

changes direction from southeasterly to southwesterly when it approaches the Indian sub-continent. The Arabian Sea (AS) is warmer during this period associated with higher sea level. The lower SSHA at the south is due to the northward advection of cold water. The low SST and the low sea level at the southwest coast of India indicates upwelling while the coastal waters of the east coast are abnormally warm with higher SSHA, a characteristic normally associated with sinking. The wind and SST support the existence of a strong upwelling zone near the coast of Somali during the summer months while the positive sea level anomaly opposes it. The patch of high sea level along the equator from 70°-90°E during April-June is an indication of strong eastward flow often referred to as the Equatorial Jet (Wyrki 1973; Muraleedharan and Prasannakumar, 1992, Muraleedharan, 1993). A similar feature is not seen during the post-monsoon transition (Oct-Nov). We presume that the pre-monsoon transition jet (Wyrki Jet) is strictly an annual phenomenon while the post-monsoon jet has strong inter-annual variability.

The wind pattern over the tropical Indian Ocean during winter is analogous to the other oceans, with North-East and South-East trade winds on either side of the equator. The equatorial current system of the Indian Ocean appears to be displaced to the south as the north

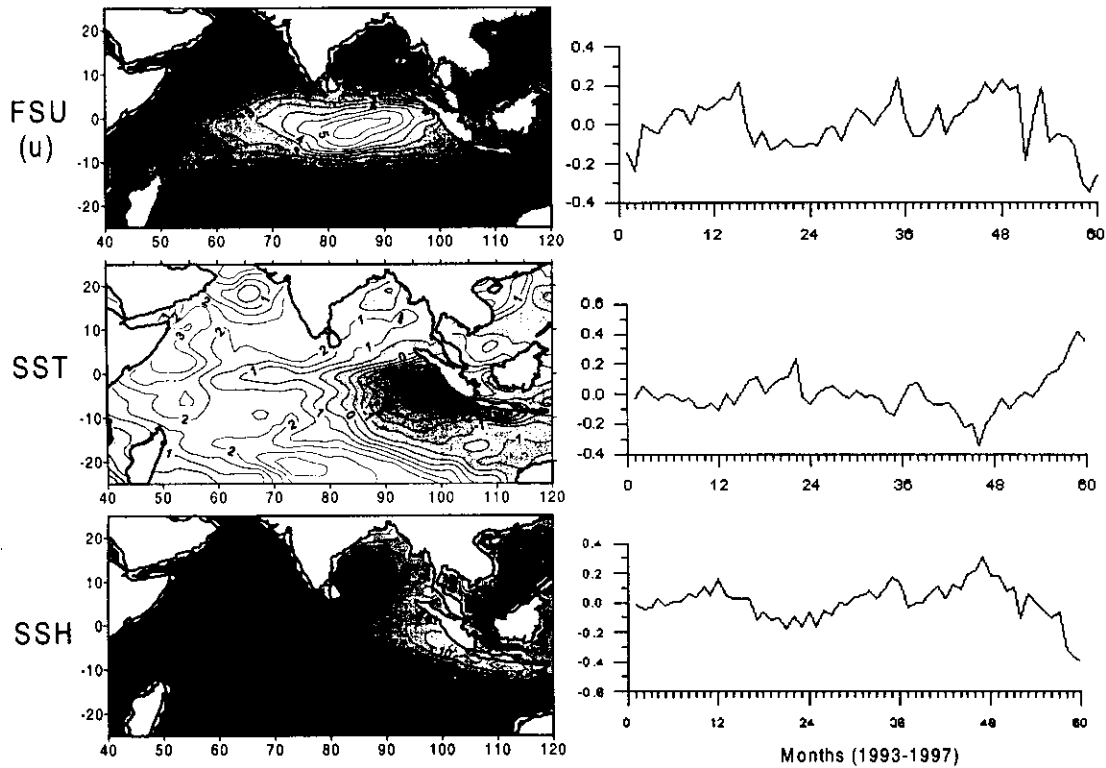


Fig. 2. First spatial (left panel) and temporal (right panel) EOF mode of non-seasonal deviation data. U-component of the wind speed (upper panel), Sea Surface Temperature (middle panel) and Sea Surface Height Anomaly (bottom panel).

is landlocked. The SST of AS and BB decreases when winter sets in (Nov.-Feb) along with warming at the south (southern summer). This cooling and warming is supported by the low and high sea level anomalies, respectively.

### 3.3 Inter-annual signature

The primary EOF mode of the non-seasonal deviation data set of the parameters is displayed in Fig. 2. The spatial distribution of the zonal wind pattern indicates strong westerlies over the equator whose core is centered around 80°-90°E, close to the coast of Sumatra (top panel of Fig. 2). A patch of easterlies is noticed near the Somali Coast. The variation of this spatial structure with time is plotted as normalized amplitude over a period of 5 years (top right panel in Fig. 2). It is interesting to note that the westerlies do exist over the equator during the months of October-November in 1993, 1995 and 1996 but not in 1994 and 1997. On the contrary, easterlies started appearing in 1994 and 1997 along the equator during the entire later half of the year. The strength of these easterlies reaches to a maximum in 1997.

The spatial and temporal mode of SST reveal the anomalous warming and cooling of the equatorial Indian Ocean (middle panel of Fig. 2). The temporal distribution of spatial variability hardly crosses zero except during 1994 and 1997, indicating warming near

Sumatra and cooling off Somali (middle right panel of Fig 2). The entire pattern however changes in 1994 and 1997 where we come across anomalous cooling off Sumatra and warming off Somali. The process occurring in 1997 is much stronger than in 1994, as shown by the temporal variability curve.

The spatial variability of SSHA, as shown by the significant mode, is dominated by high sea surface close to the coast of Sumatra and low sea surface around 8°S between 60° and 80°E (lower panel of Fig.2). The variability of this spatial structure with time is presented in the lower right panel of Fig. 2. High SSHA values at Sumatra and low values at the south are analogous to the warming and cooling occurring at these regions during the years 1993, 1995 and 1996. In 1994 and 1997 the SSHA values are at their lowest off Sumatra and highest at 8°S. The sea surface height difference during 1997 is much larger in comparison to the year 1994.

The spatial and temporal variability of WS, SST and SSHA suggests the presence of a dipole system at the equatorial Indian Ocean as observed by Shaji et al. (1999) during 1994 and 1997. Although Shaji et al. (1999) and Webster et al. (1999) describe this phenomenon as an expression of an internal dynamics and that its co-existence with the El Nino event is a coincidence, we still believe that its relationship with El Nino events that occurred in 1994 and 1997 cannot be ruled

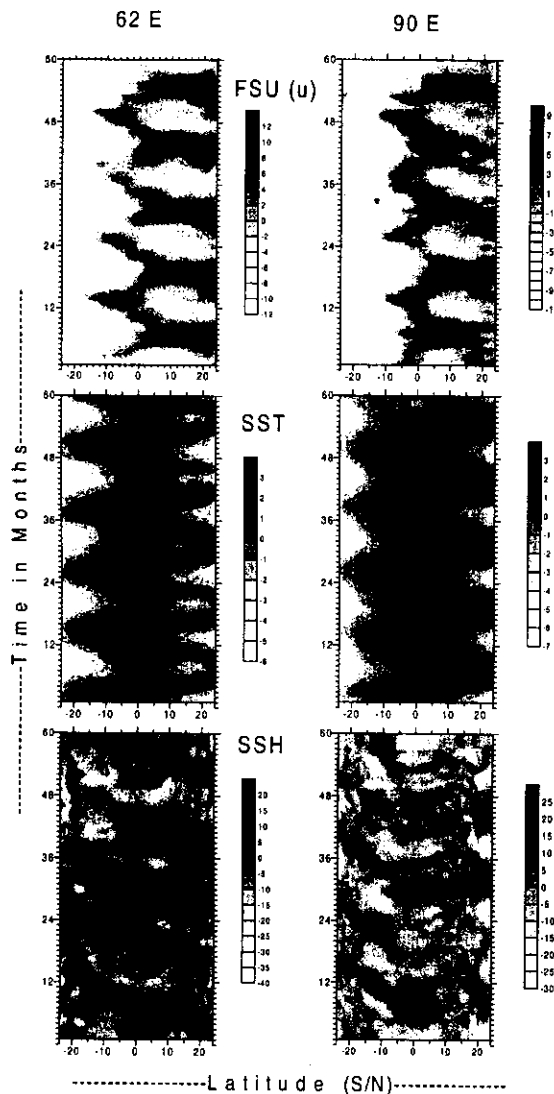


Fig. 3. Time-latitude sections of the U-component of the Wind Speed (top panel), Sea Surface Temperature (middle panel) and Sea Surface Height Anomaly (bottom panel) at 62°E (left panel) and 90°E (right panel).

out. Chambers et al. (1999) also believe in the coincidence of inter-annual warming with a frequency similar to that of El Niño. He has evidence to suggest that the warming begins with wind-forced Rossby waves in the southeastern Indian Ocean associated with the southern oscillation. This led us to believe that the change of westerlies to easterlies at the equatorial Indian Ocean is triggered by the southern oscillation occurring at the southeastern Indian Ocean. This reversed wind pattern intensifies the Ekman pumping mechanism close to the coast of Sumatra by inducing offshore drift. This process brings cold subsurface water to the surface. The warm surface water is carried by the wind to the west, which would probably produce anomalously warm surface water at the west. The stronger the southern oscillation and the El Niño, the faster will be the easterlies. Strong easterlies can

generate vigorous upwelling west of Sumatra. This can explain the colder SST anomaly during 1997. The SSH also changes with change in SST. It is surprising to note that the colder/warmer water at the west does not coincide with the lower/higher sea surface height. The anomalous SSH is observed slightly south of the equator between 60° and 80°E. Chambers et al. (1999) also observed a similar shift in the high sea level region from the warming zone.

### 3.4 Time-latitude sections

Two trans-equatorial sections of zonal component of the WS, SST and SSHA were selected at 62°E and 90°E from 25°N to 25°S to prepare the time-latitude sections for understanding the inter-annual variability (Fig. 3). The zonal wind component at 62°E and 90°E indicates westerlies in the northern hemisphere during the monsoon season (June-Sept) and easterlies in the southern hemisphere (top panel in Fig. 3). The easterlies appear to be propagating from 10°S (in January) to the equator (Apr-May) and form the monsoon wind drift while it again bifurcates in October and propagates to the south. This meridional oscillation of westerlies will generate the equatorial jet (Wyrtki, 1973) when it passes the equator during April-May and October-November (Fig.3 & Fig.1). The figures show that this oscillation is more at 62°E than at 90°E and the westerlies at 62°E moved to the northern hemisphere when easterlies prevail at the equator. It is observed that this shifting at 62°E is from 15°S to 5°N whereas it moves from 10°S to 2°N at 90°E. This is perhaps due to the monsoon wind from south which enters the northern hemisphere through the western equatorial India Ocean and changes direction to southwesterlies. The inter-annual variability of these propagating westerlies is evident in the figures presented. This variability is quite significant during 1994 and 1997, especially at 90°E (Fig. 3, upper panel). The pre-monsoon bifurcation of the westerlies which produce the pre-monsoon equatorial jet has less inter-annual variability whereas the post-monsoon westerlies (which produce post-monsoon equatorial jet) seem to be absent during 1994 and 1997 as these years are prone to El Niño events. The absence of post-monsoon westerlies might be an indication of the ocean preparing itself for a dipole structure.

The variation of SST anomaly with time at 62°E and 90°E is presented in the middle panel of Fig. 3. Cooling and warming at the south is associated with advection of water from high latitude during southern winter (June-Sept.) and the spreading of equatorial warm water to south during austral summer (Nov-Feb), respectively. At the north, along 62°E, the patches of cold water centered around 17°N in the summer months

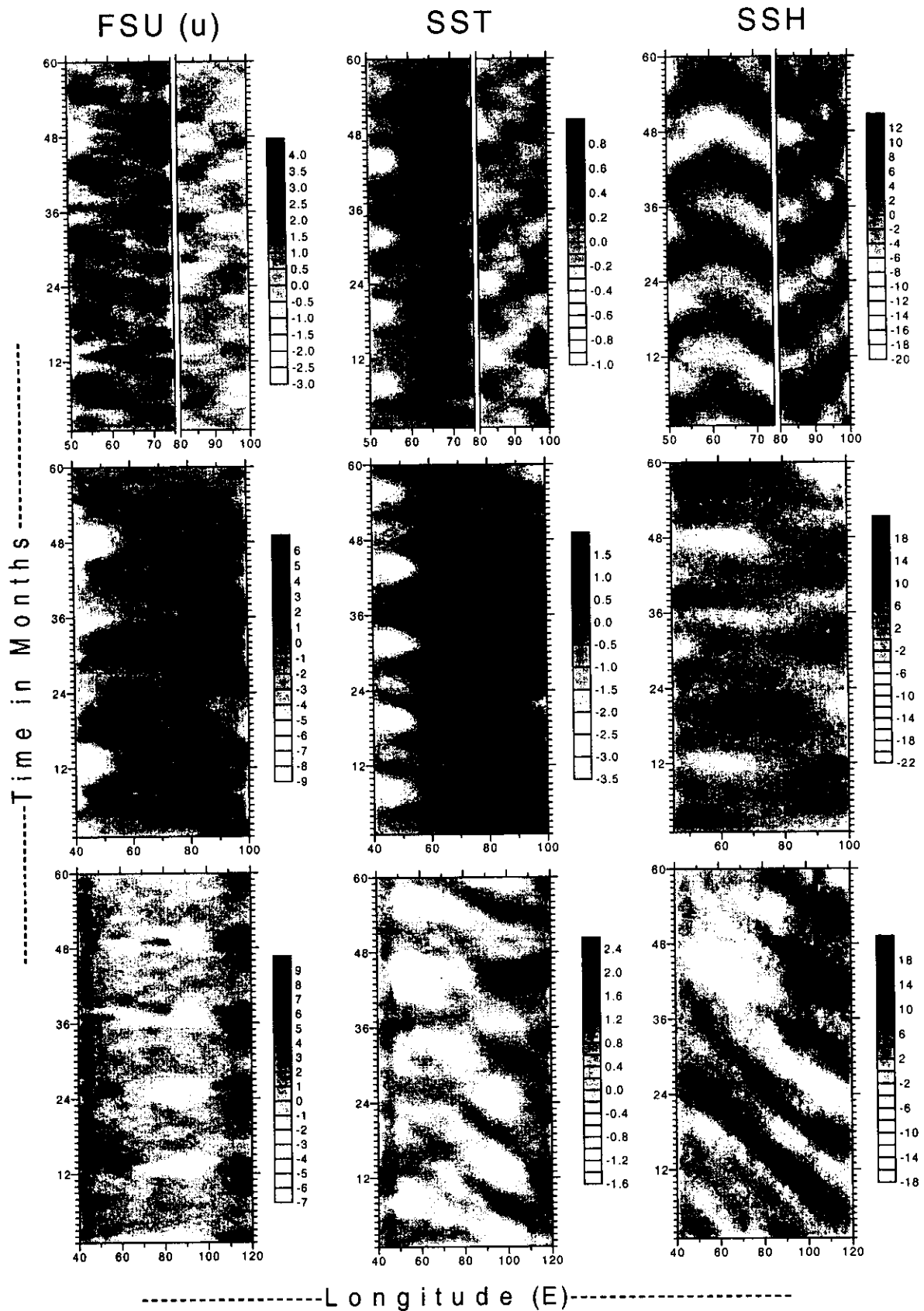


Fig. 4. Time-longitude section of the U-component of the Wind Speed (left panel), Sea Surface Temperature (middle panel) and Sea Surface Height Anomaly (right panel) between 10°-15°N (top panel), 2.5°N-2.5°S (middle panel) and 10°-15°S (bottom panel).

are due to the open ocean upwelling induced by the Findlater Jet (Bauer et al. 1991). The winter cooling mechanism activated during winter is responsible for the cold patch at 24°N (Prasannakumar and Prasad, 1996). There are not many features observed at the eastern section.

The time-latitude section of SSHA at 62°E and 90°E exhibits a strip of high values during both the monsoon months (May-Aug) and postmonsoon months (Oct-Nov), right from 15°N (bottom panel in Fig. 3). It appears that the high sea levels are associated with westerly winds which are present at the equator during two transition months viz; April-May and October-November. These westerlies generate the Equatorial Jet that causes accumulation of warm water towards the equator, a process associated with equatorial downwelling (Wyrtki, 1973; Muraleedharan, 1993). The accumulation of warm water produces high sea level which is depicted here. This process is more conspicuous at 90°E than at 62°E. The demarcation of two highs is more pronounced during 1993, 1995 and 1996 while during 1994 and 1997 the highs during the postmonsoon transition period appear to be vanishing (bottom right panel in Fig 3). This establishes the relationship of these highs with the prevailing westerlies along the equator. This interannual variability is again attributed to the southern oscillation and El Nino. There is another interesting pattern observed at both 62°E and 90°E. The sea surface heights are propagating from the equator to the south (25°S) along these two longitudes. The propagation is more prominent at 90°E. It is believed that the meridional oscillation of the westerlies from the equator to the south is the driving force of this oceanic response. The southward propagation of the sea surface height continues even after the wind subsides.

### 3.5 Time-longitude sections

Time-longitude sections of zonal WS, SST anomaly and SSHA are plotted at three locations viz., north (10°-15°N), equator (2.5°N-2.5°S), south (10°-15°S) in Fig. 4. The wind over Arabian Sea and Bay of Bengal seems to be reversing twice a year. While the SST anomaly over the Arabian Sea fails to indicate any surface expression, it shows a west to east propagating signal over the Bay of Bengal. The SSHA over the Arabian Sea may be due to the combination of westward propagating Rossby wave and eastward propagating Kelvin wave. On the contrary, the pattern of SSHA over the Bay of Bengal is more or less similar to the Kelvin wave propagation (top right panel in Fig. 4). The changing wind pattern over the equatorial Indian Ocean again fails to produce any impact on the sea surface. The SST and SSH do not produce any kind of propagating signal at

the equatorial region. A strong evidence of Rossby wave propagation is seen in the section of SST anomaly and SSHA over the southern latitude (10°-15°S, bottom middle and right panel in Fig. 4).

### Acknowledgements

The authors are thankful to the Director, NIO for providing facilities for undertaking this work. We also thank Dr. Mahadevan, Emeritus Scientist, NIOT, Chennai and Mr. Rama Rao for their help in modifying the EOF program. This is NIO contribution No. 3594.

### References

- Anderson, D.L.T., and P.W. Rowlands, 1976, The role of inertia-gravity and planetary waves in the response of a tropical ocean to the incidence of an equatorial Kelvin wave on a meridional boundary. *J. Mar. Res.*, 34, 295-312.
- Bauer, S, G.L. Hitchcock and D.B. Olson, 1991, Influence of monsoonally forced Ekman dynamics of upper surface layer depth and phytoplankton bio mass distribution in the Arabian Sea. *Deep Sea Res.*, 38, 531-553.
- Chambers, D.P., J.C., Ries, C.K. Shum and B.D. Tapley, 1998, On the use of tide gauges to calibrate altimeter drift, *J. Geophys. Res.*, 103, 12,885-12,890.
- Chambers, D.P., B.D. Tapley and R.H. Stewart, 1999, Anomalous warming in the Indian Ocean coincident with El Nino. *J. Geophys. Res.*, 104 (C2), 3035-3047.
- Cheney, R., L. Miller, R. Agree, N. Doyle and J. Lilligrige, 1994, TOPEX/POSEIDON. The 2 cm solution. *J. Geophys. Res.*, 99, 24,555-24,564.
- Clarke, A.J., 1983, The reflection of equatorial waves from oceanic boundaries, *J. Phy. Oceanogr.*, 13, 1193-1207.
- Goldenberg, S.B. and J.J. O'Brien, 1981, Time and Space variability of tropical Pacific wind stress, *Mon. Wea. Rev.*, 109, 1190-1207.
- Johnson, M.A., and J.J. O'Brien, 1990, The north east Pacific Ocean response to the 1982-83 ElNino, *J. Geophys. Res.*, 95, 7155-7166.
- Moore, D.W, 1968, *Planetary-gravity waves in an equatorial ocean*. Ph.D dissertation, 207 p., Harvard Univ., Cambridge, Mass.
- Muraleedharan, P.M, 1993, Intermonsoonal Equatorial Jets. *Indian J. Marine Sci.*, 22, 1-7.
- Muraleedharan, P.M and S. Prasannakumar, 1992, Equatorial Jet - A case study. *Indian J. Marine Sci.*, 4211, 35-45.
- Prasannakumar, S. and T.G. Prasad, 1996, Winter cooling in the northern Arabian Sea. *Current Sci.*, 71, 834-841.
- Rao, R.R., R.L. Molinari and J.F. Festa, 1989, Evaluation of the climatological near surface thermal structure of the tropical Indian Ocean, description of mean monthly mixed layer depth, sea surface temperature, surface current and surface meteorological fields. *Geophys. Res.*, 94, 10,801-10,815.
- Reynolds, R.W and T.M. Smith, 1994, Improved global sea surface temperature analysis, *J. Climate*, 7, 929-948.
- Shaji, N.H., B.N. Goswami, P.N. Vinayachandran and T. Yamagata, 1999, A dipole mode in the tropical Indian Ocean, *Nature*, 401, 360-363.
- Shenoi, S.S.C, D. Shankar and S.R. Shetye, 1999, On the sea surface temperature high in the lakshadweep sea before the onset of the sw monsoon. *J. Geophys. Res.*, 104 (c7), 15,703-15,712.
- Webster, P.J., A.M. Moore, J.P. Loschnigg and R.R. Leben, 1999, Coupled ocean-atmosphere dynamics in the Indian Ocean during 1997-98, *Nature*, 401, 356-360.
- Wyrtki, K., 1973, An equatorial Jet in the Indian Ocean. *Science*, 181, 262-264.